

## STRUCTURAL AND OPTICAL CHARACTERISTICS OF POLY(VINYL ALCOHOL)/ CARBOXYMETHYL CELLULOSE/CURCUMIN NANOCOMPOSITES

E. Ahmed<sup>1</sup>, A. Aboelkhair<sup>2</sup> and A.M. Abdelghany<sup>3\*</sup>

<sup>1</sup>Chemistry Department, Faculty of Biotechnology, Badr University in Egypt, New-Cairo,  
11829, Egypt

<sup>2</sup>Chemistry Department, Faculty of Science, Mansoura University, Mansoura, Egypt

<sup>3</sup>Spectroscopy Department, Physics Research Institute, National Research Centre,  
33 El-Behouth St., Dokki, 12311, Giza, Egypt

(Received November 30, 2021; Revised January 2, 2022; Accepted January 3, 2022)

**ABSTRACT.** Curcumin nanoparticles (CurNP's) were successfully synthesized, characterized, and used as a cross-linking dopant of polyvinyl alcohol/ sodium carboxymethyl cellulose (PVA/CMC) semi-natural polymer blend. Synthesized nanocomposite films of (PVA/CMC/CurNP's) were characterized using Fourier transforms infrared FTIR spectroscopy and tested for their resistance of different bacterial grams. Obtained data shows that studied PVA polymerized and cross-linked with CMC as a result for hydrogen bonding between the carboxylic groups and with the non-substituted hydroxyl groups of the cellulose molecule. The optical energy gap was found to be sensitive for the CurNP's doping level, and the indirect transition was dominant in the studied samples. The addition of CurNP's appears to increase the activity index of all samples against both gram-negative and positive bacteria, and their activity increases with increasing dopant level until a specific optimal concentration.

**KEY WORDS:** Curcumin nanoparticles, Semi-natural polymer blend, Antibacterial, FTIR, Optical energy gap

### INTRODUCTION

Curcumin is an enormously influential, non-toxic, bioactive agent found in turmeric and has been known for centuries as a household remedy to many ailments. The only detriment is that it suffers of low aqueous solubility and poor bioavailability. Nanoparticles of curcumin (nano curcumin) were prepared by a procedure based on a wet-milling approach. They were found to have a fine particle size distribution in the range of 240nm. On the contrary to curcumin, nano curcumin was found to be freely dispersible in water in the absence of any surfactants. The chemical structure of nano curcumin was the same as that of curcumin, and there was no modification during nanoparticle preparation. A minimum restrained concentration of nano curcumin was determined for various bacterial and fungal strains and was compared to that of curcumin. Curcumin, the agent responsible for the characteristic yellow-orange color and the solid spicy taste of curries, is the principal polyphenol derived from the root of the turmeric plant (*Curcuma longa*). In addition to its uses in the food industry as a spice and food-coloring agent, curcumin has commonly been used as an herbal remedy for inflammatory disorders, such as arthritis, colitis, and hepatitis. Former research has revealed that curcumin possesses pharmacological effects, including anti-tumor, anti-inflammatory, and anti-infectious activities [1-4].

Cellulose is the largest polymer on earth, which, as well as the most common organic compound. The bulk of cellulose is commonly used in manufacturing paper and cardboard goods like raw material, and a limited fraction is used in the manufacture of commodity materials and value-added carboxymethyl cellulose and methylcellulose, etc. [5]. In addition, by-products such as carboxymethyl cellulose, methylcellulose, ethylcellulose, hydroxypropyl cellulose, cyanoethyl cellulose, and so on can be chemically modified to pay for value-added cellulose in all these cellulosic products that are converted. Because of its broad commercial applications concerning

\*Corresponding author. E-mail: a.m\_abdelghany@yahoo.com

This work is licensed under the Creative Commons Attribution 4.0 International License

volume demand, CMC is synthesized in substantial quantities. A wide variety of uses, including food additives, pharmaceuticals, cosmetics, papers, adhesives, lithography, ceramics, detergents, and fabrics, are recognized within numerous industries [6, 7]. In all cellulose ether product groups, CMC is one of the largest market shareholders with such diverse applications along with its low pricing. Carboxymethyl cellulose (CMC) is a type of cellulose ether that is soluble in water. It is one of the essential cellulose derivatives produced in the presence of an alkali catalyst by reacting cellulose with acetic acid. Due to its hydrophilicity, non-toxicity, excellent biocompatibility, and low price, CMC has outstanding pharmaceutical and biomedical applications. However, the electrospinning of CMC is highly difficult due to the very poor solubility of organic solvents. The CMC nanofibers were successfully manufactured in previous studies by combining them with polymers such as polyethylene oxide (PEO), poly (vinyl alcohol) (PVA) [8, 9].

Poly(vinyl alcohol) (PVA) is a water-soluble polyhydroxy polymer, used in practical applications because of its simple preparation, excellent chemical resistance and physical properties, ideal mechanical properties, and is fully biodegradable and inexpensive. The -OH groups can be a source of hydrogen bonding (H-bonding) and thus assist in polymer blend forming. There are excellent film formation, emulsifying, and adhesive properties of polyvinyl alcohol. It is oil, grease, and soap resistant as well. It is odorless, non-toxic, with high tensile strength, flexibility, and high resistance to oxygen and scent. Owing to the desirable nature of comparatively small -OH groups bound to alternate carbon atoms of PVA, the chemical composition of PVA favors the development of intramolecular hydrogen bonding, so it is used in the preparation of different membranes and hydrogels [10].

The presented study aims to introduce a clear insight into the role of curcumin nanoparticles in the physical characteristics of CMC/PVA cross-linked polymer blend and their correlation with their bioactivity against pathogenic grams.

## EXPERIMENTAL

Polyvinyl alcohol (PVA) of molecular weight 6000 g/mol supplied by Acros Organics (USA) in combination with sodium carboxymethyl cellulose (CMC) provided by Lanxess (Germany) were used for blend biofilm preparation. Curcumin from (*Curcuma longa*) was supplied by herbal house centers (Egypt). Curcumin nanoparticles were prepared using hydrothermal route adopting 2 g curcumin powder with 2 mL dimethylsulfoxide (DMSO) with 30 mL bidistilled water at 60 °C for about 12 h.

The eco-friendly solvent casting route was used for the preparation of blend films and other nanocomposite films doped with CurNP's adopting water as a common solvent. Calculated amounts of both polymers were dissolved separately in deionized water with vigorous stirring at room temperature. The two solutions were mixed, and appropriate amounts of CurNPs were added, as shown in table (1). Obtained viscous solutions were poured in a polypropylene Petri-dishes and positioned in a 50 °C regulated oven until evaporation of all solvent traces.

Table 1. Sample nomination and composition.

Sample	CMC	PVA	CurNP's
	wt/wt		ml/wt
PVA	0.0	100	0.0
CMC	100	0.0	0.0
Blend	70	30	0.0
B1Cur	70	30	1.0
B2Cur	70	30	2.0
B5Cur	70	30	5.0
B7.5Cur	70	30	7.5
B10Cur	70	30	10.0

Function groups of the studied films were investigated using (Nicolet is 10) single-beam spectrophotometer within the mid-range between 4000-400  $\text{cm}^{-1}$ . UV/Vis. Electronic spectral data were recorded using JASCO V-570 double-beam spectrometer. The size and morphology of synthesized nanoparticles were investigated using the JEOL-JEM-1011 transmission electron microscope (TEM).

## RESULTS AND DISCUSSION

### *Characterization of synthesized nano curcumin*

UV/Vis. optical absorption spectrum of synthesized curcumin shown in Figure 1 reveals the appearance of a strong UV absorption band located at 220 nm attributed by several authors to the presence of iron impurities in the extract even at ppm-level. Such a peak followed by another peak in the same region at about 350 nm is generally assigned and confirms the presence of organic chromospheres within the extract [11, 12]. Besides, such peaks can be related to unsaturated groups and heteroatoms such as sulfur, nitrogen, and oxygen.

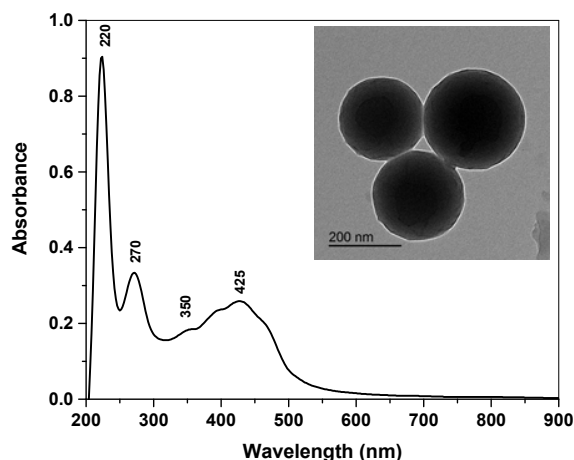


Figure 1. UV/Vis. optical absorption spectrum and TEM micrograph of synthesized curcumin nanoparticles.

The spectrum also shows a visible broad band centered at 425 nm attributed to the formation of curcumin in the nano-form with a shoulder at about 470 nm in their descending lobe. It is well known that bulk curcumin showed a visible absorption band at 450 nm [12], which means that nano curcumin usually shows a blue shift. Transmission electron microscopic images approve the formation of spherical CurNP's with a radius of about 65 nm.

### *FT-IR optical absorption spectra of studied materials*

FTIR can reveal the chemical changes by producing absorption spectrum. It can be seen that FTIR spectra of original curcumin and curcumin nanoparticles did not show significant differences. Infrared spectrum of curcumin showed its signature peaks at 3508  $\text{cm}^{-1}$  (phenolic O-H stretching vibration), 1628  $\text{cm}^{-1}$  (aromatic moiety C=C stretching), 1597  $\text{cm}^{-1}$  (benzene ring stretching)

vibrations),  $1509\text{ cm}^{-1}$  (C=O and C=C vibrations),  $1428\text{ cm}^{-1}$  (olefinic C-H bending vibrations),  $1278\text{ cm}^{-1}$  (aromatic C–O stretching vibrations),  $1024\text{ cm}^{-1}$  (C–O–C stretching vibrations) [13].

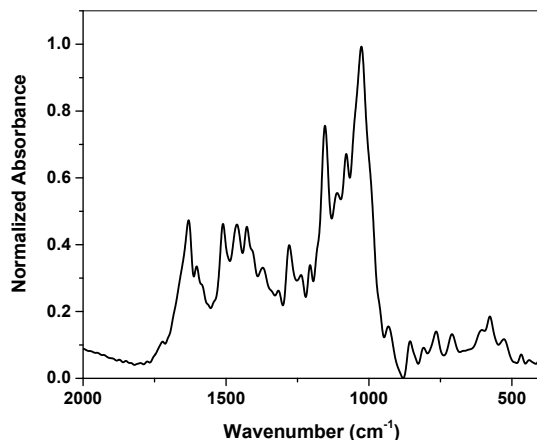


Figure 2. FTIR spectrum of synthesized curcumin nanoparticles.

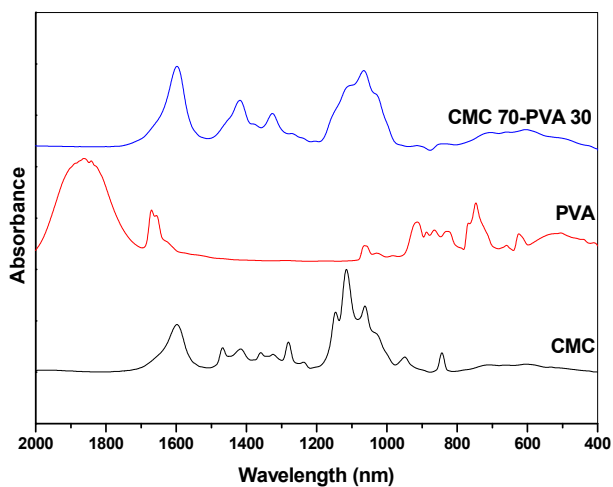


Figure 3. FTIR absorption spectra of pristine PVA, CMC homopolymer in combination with their cross-linked PVA/CMC blend films.

Figure (3) reveals FTIR absorption spectra of pristine PVA, CMC homopolymer in combination with their cross-linked PVA/CMC blend films. Polyvinyl alcohol spectral curve shows characteristic bands reported by different authors [14-16]: (i) a broad medium intensity band at  $3340\text{ cm}^{-1}$  was assigned to the hydroxyl group in the main structure, (ii) a sharp, intense band at  $1735\text{ cm}^{-1}$  and another band at  $1100\text{ cm}^{-1}$  corresponds to the C-O stretching vibrations in the acetate group, (iii) bands at  $2940$  and  $2910\text{ cm}^{-1}$  attributed for the aliphatic backbone C–H

stretching vibrations and (iv) the band at  $1335\text{ cm}^{-1}$  has been assigned to the combination frequencies of (CH·OH).

Additionally, the spectrum of the CMC sample shows the following absorption bands: The band located at about  $2980\text{ cm}^{-1}$  was assigned for C–H stretching vibrations. The band at  $1185\text{ cm}^{-1}$  attributed for C–O stretching vibrations of ether groups results from carboxymethylation of cellulose or ether linkage of cellulose compartment in combination with that arising from the two types of ether present in CMC. A strong band at  $3223\text{ cm}^{-1}$  results from O–H stretching of the non-substituted hydroxyl groups of cellulose. The band located at  $816\text{ cm}^{-1}$  attributed to the C–O stretching of alcohol. Two broad bands initially located at  $3225$  and  $3495\text{ cm}^{-1}$  are correlated with intramolecular hydrogen bonding in CMC sodium salt molecules [17-19].

Finally, FTIR of cross-linked polymer blend shows notable variations in the spectral bands resulting from PVA polymerization and increase in the hydrogen bonding result in a broadness of the band extended from  $3000$  to  $3600\text{ cm}^{-1}$ . The previous may explain the formation of hydrogen bonding between the carboxylic groups themselves and with the non-substituted hydroxyl groups of the cellulose molecule. Therefore, it was suggested that interaction of such blend might be assigned to hydrogen bonding.

Figure 4 reveals FTIR absorption spectra of pristine synthesized CurNP's dopant with CMC/PVA cross-linked blend films. It was suggested that CurNP's could interact with both CMC and/or PVA causing cross-linking of the polymeric matrix as indicated in Scheme 1.

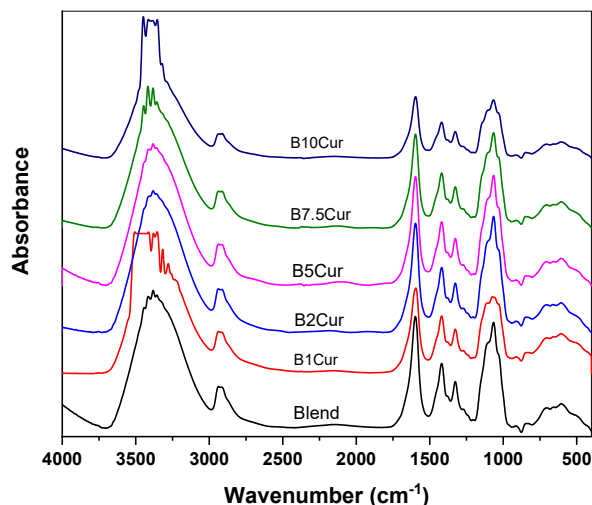
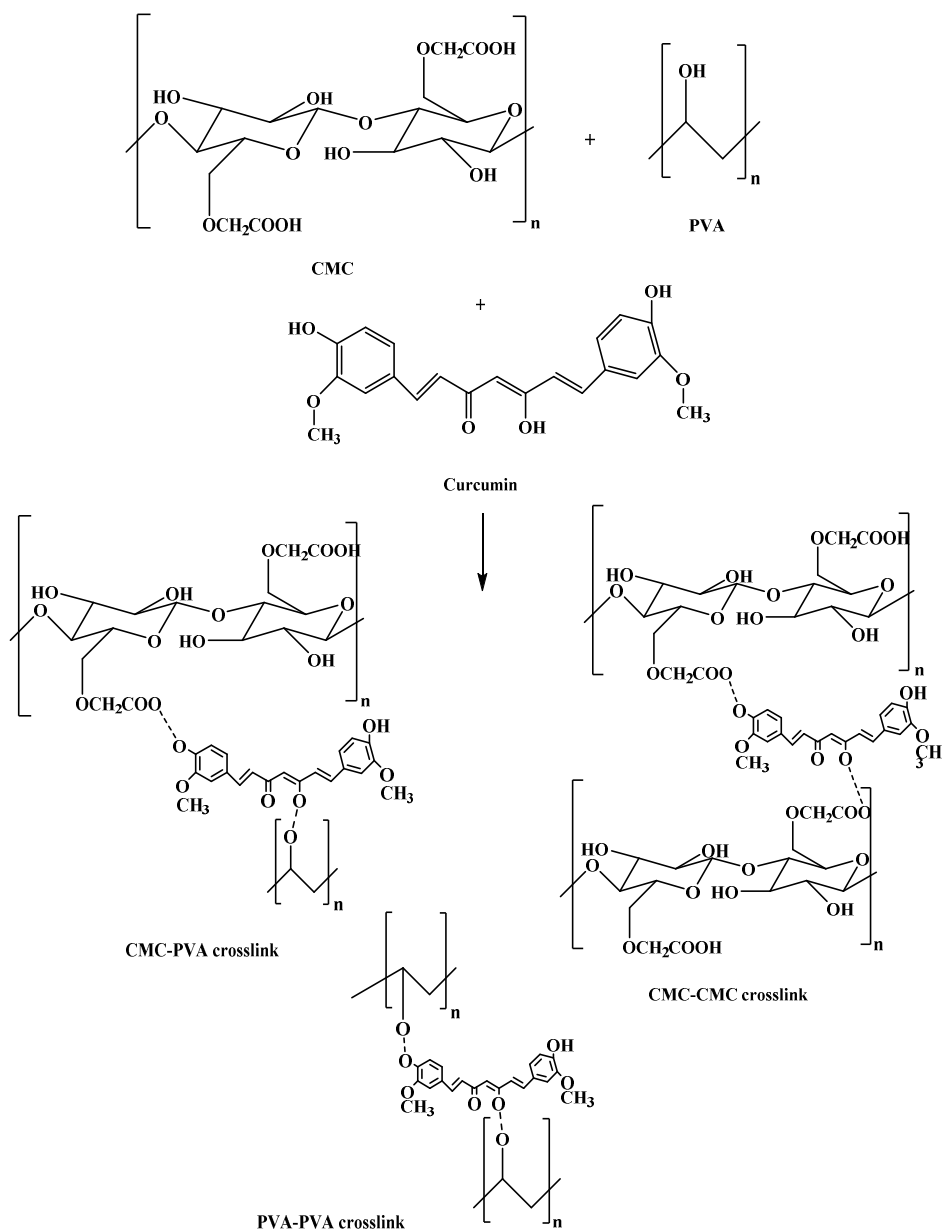


Figure 4. FTIR absorption spectra of pristine synthesized CurNP's dopant with CMC/PVA cross-linked blend films.

#### UV/Visible electronic transitions

Figure 5 shows UV/Vis. optical transition of CMC/PVA poly-blend and their nanocomposites with curcumin nanoparticles. The spectra of studied samples show an absorption band in the UV range at about  $220\text{ nm}$  with a fundamental edge in the vicinity of  $250\text{ nm}$  attributed for  $n\rightarrow\pi^*$  transition [20, 21].



Scheme 1. Suggested interaction of CurNp's with both CMC and PVA.

Two major observations were recorded with the addition of CurNP's. Obtained spectral data show maintenance of the bands at the UV region without a change in their position. The observed band in the visible region shows broadness and increasing intensities with increasing curcumin content combined with splitting in the observed shoulders attributed to the hydrogen bonding and interactions between polymeric matrices and dopant material. Mode of transition can be estimated from analysis of the optical band gap calculated from both fundamental absorption edge ( $E_g = hc/\lambda$ ) or via Tauc's plots of energy ( $h\nu$ ) versus  $(\alpha h\nu)^{1/2}$  or  $(\alpha h\nu)^2$  for both direct and indirect energy gap respectively. Figure 6 shows Tauc's plot and their use for the estimation of optical energy gap from their extrapolated lines. The estimated energy gap for the blend sample and their nanocomposites containing different content of curcumin nanoparticles were listed in Table 2.

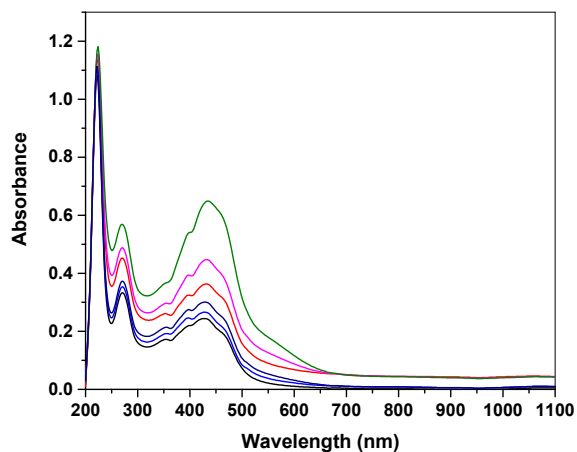


Figure 5. UV/Vis. optical spectra of CMC/PVA poly-blend and their nanocomposites with different curcumin nanoparticles content.

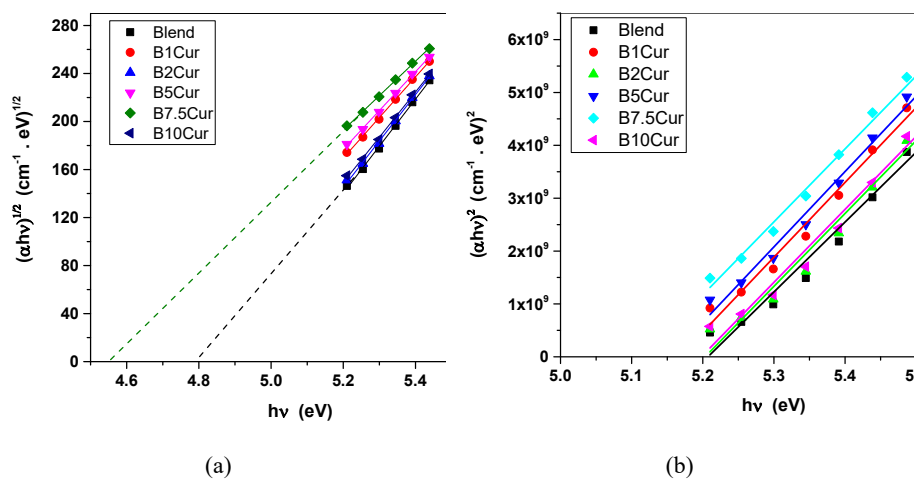


Figure 6. Tauc's plots of the studied samples.

Table 2. Estimated energy gap with a different curcumin content.

Samples	$\lambda_{\text{edge}}$	$E_{\text{opt}}$	$E_{\text{Indirect}}$	$E_{\text{Direct}}$
	nm			
Blend	256	4.8	4.80	5.27
B1Cur	243	5.1	4.70	5.20
B2Cur	256	4.6	4.80	5.26
B5Cur	281	4.4	4.50	5.20
B7.5Cur	286	4.3	4.59	5.15
B10Cur	279	4.4	4.80	5.25

### Antibacterial tests

Antimicrobial activity tests of studied nanocomposite films were tested against different pathogenic grams. Two streams of each gram were studied, gram-positive (*B. subtilis* and *S. aureus*) and gram-negative (*E. coli* and *P. aeruginosa*) bacteria are shown in Figure 7. The experiment was conducted at pH 7 and 37 °C with distilled water and compared with that free of dopant nanoparticles [22]. Antimicrobial resistance against various grams can be interpreted in terms of three different mechanisms: enzymatic breakdown of antibacterial medications, changes in antimicrobial target bacterial proteins, and changes in antibiotic membrane permeability.

The relation between curcumin nanoparticles content (mL/wt) drawn against the diameter of inhibition zone (mm) reveals three important facts: (1) the inhibition zone of samples containing curcumin nanoparticles shows a larger inhibition zone compared with a pure blend (70CMC/30PVA), (2) the increase of CurNP's content is usually combined with an increase in the inhibition zone, (3) higher concentrations 7.5 and 10 shows a gradual and small variation, and (4) Gram-negative bacteria usually show higher activity.

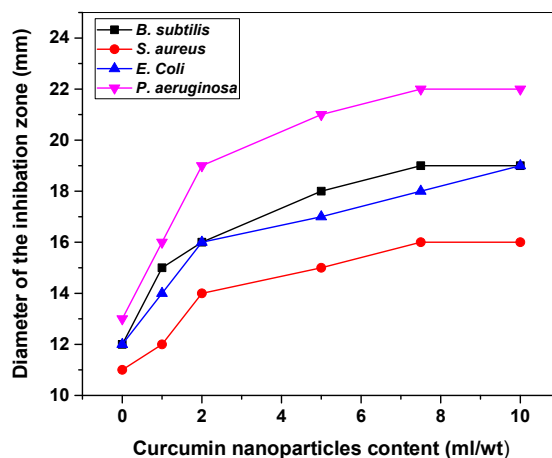


Figure 7. Relation between curcumin nanoparticles content (mL/wt) drawn against the diameter of inhibition zone (mm).

### CONCLUSION

Curcumin nanoparticles (CurNP's) were successfully synthesized from *Curcuma longa* using a solvent-free hydrothermal route. The formation of CurNP's was approved via the formation of a

visible band located at 425 nm while transmission microscope micrographs indicate the formation of spherical CurNP's with a radius of about 65 nm. Synthesized CurNP's were used as a dopant cross-linker for PVA/CMC nanocomposite films. Synthesized films were observed to be sensitive for the CurNP's doping level especially in the visible region and the indirect transition was dominant. Samples containing CurNP's shows higher biological activity against different pathogenic grams with respect to the undoped polymer blend while higher concentrations 7.5 and 10 show gradual and small differences and gram-negative bacteria usually show higher activity.

## REFERENCES

1. Zhao, Z.; Xie, M.; Li, Y.; Chen, A.; Li, G.; Zhang, J.; Li, S. Formation of curcumin nanoparticles via solution-enhanced dispersion by supercritical CO<sub>2</sub>. *Int. J. Nanomed.* **2015**, *10*, 3171. DOI: 10.2147/IJN.S80434.
2. Chopra, M.; Jain, R.; Dewangan, A.K.; Varkey, S.; Mazumder, S. Design of curcumin loaded polymeric nanoparticles-optimization, formulation and characterization. *J. Nanosci. Nanotechnol.* **2016**, *16*, 9432-9442.
3. Chen, X.; Zou, L.Q.; Niu, J.; Liu, W.; Peng, S.F.; Liu, C.M. The stability, sustained release and cellular antioxidant activity of curcumin nanoliposomes. *Molecules* **2015**, *20*, 14293-14311.
4. Ismail, E.H.; Sabry, D.Y.; Mahdy, H.; Khalil, M.M.H. Synthesis and characterization of some ternary metal complexes of curcumin with 1,10-phenanthroline and their anticancer applications. *J. Sci. Res.* **2014**, *6*, 509-519.
5. Dufresne, A.; Nanocellulose processing properties and potential applications. *Curr. For. Rep.* **2019**, *5*, 76-89.
6. Carlmark, A.; Larsson, E.; Malmström, E. Grafting of cellulose by ring-opening polymerisation—A review. *Euro. Polym. J.* **2012**, *48*, 1646-1659.
7. Durand, H.; Smyth, M.; Bras, J.; Nanocellulose: A new biopolymer for biomedical application. *Biopolymers for Biomedical and Biotechnological Applications*, **2021**; pp. 129-179.
8. Badry, R.; El-Khodary, S.; Elhaes, H.; Nada, N.; Ibrahim, M. Optical, conductivity and dielectric properties of plasticized solid polymer electrolytes based on blends of sodium carboxymethyl cellulose and polyethylene oxide. *Opt. Quantum Electron.* **2021**, *53*, 1-15.
9. Saadiah, M.A.; Kufian, M.Z.; Misnon, I.I.; Samsudin, A.S. Electrochemical properties of CMC-PVA polymer blend electrolyte for solid state electric double layer capacitors. *J. Electron. Mater.* **2021**, *50*, 303-313.
10. Madhumanchi, S.; Srichana, T.; Domb, A.J. *Polymeric Biomaterials in Biomedical Materials*, Springer: Cham; **2021**; pp. 49-100.
11. Jain, P.K.; Soni, A.; Jain, P.; Bhawsar, J. Phytochemical analysis of *Mentha spicata* plant extract using UV-VIS, FTIR and GC/MS technique. *J. Chem. Pharm. Res.* **2016**, *8*, 1-6.
12. Rajasekar, A. Facile synthesis of curcumin nanocrystals and validation of its antioxidant activity against circulatory toxicity in wistar rats. *J. Nanosci. Nanotechnol.* **2015**, *15*, 4119-4125.
13. Dos Santos, R.B.; Nakama, K.A.; Pacheco, C.O.; de Gomes, M.G.; de Souza, J.F.; de Souza Pinto, A.C.; Haas, S.E.; Curcumin-loaded nanocapsules: Influence of surface characteristics on technological parameters and potential antimalarial activity. *Mater. Sci. Eng.: C* **2021**, *118*, 111356.
14. Verma, N.; Pramanik, K.; Singh, A.K.; Biswas, A. Design of magnesium oxide nanoparticle incorporated carboxy methyl cellulose/poly vinyl alcohol composite film with novel composition for skin tissue engineering. *Mater. Technol.* **2021**, 1-11. DOI: 10.1080/10667857.2021.1873634.

15. Arefian, M.; Hojjati, M.; Tajzad, I.; Mokhtarzade, A.; Mazhar, M.; Jamavari, A. A review of polyvinyl alcohol/carboxy methyl cellulose (PVA/CMC) composites for various applications. *JCC* **2020**, *2*, 69-76.
16. Abou Taleb, M.F.; Abd El-Mohdy, H.L.; Abd El-Rehim, H.A. Radiation preparation of PVA/CMC copolymers and their application in removal of dyes. *J. Hazard. Mater.* **2009**, *168*, 68-75.
17. Fessenden, R.J.; Fessenden, J.S. *Organic Chemistry*, Willard Grant Press: Boston, Mass; **1982**.
18. Al-Shamari, A.A.; Abdelghany, A.M.; Alnattar, H.; Oraby, A.H. Structural and optical properties of PEO/CMC polymer blend modified with gold nanoparticles synthesized by laser ablation in water. *J. Mater. Res. Technol.* **2021**, *12*, 1597-1605.
19. Asnag, G.M.; Oraby, A.H.; Abdelghany, A.M. Green synthesis of gold nanoparticles and its effect on the optical, thermal and electrical properties of carboxymethyl cellulose. *Composites Part B: Engineering* **2019**, *172*, 436-446.
20. Abdelghany, A.M.; Mekhail, M.S.; Abdelrazek, E.M.; Aboud, M.M. Combined DFT/FTIR structural studies of monodispersed PVP/gold and silver nano particles. *J. Alloys Compd.* **2015**, *646*, 326-332.
21. Aboelkheir, A.; Abdelghany, A.; Hanaa, D.; Abdelaal, M. Solvent free synthesis of the carboxymethyl cellulose/polyaniline silver nanoparticles composite thin films. *Egypt. J. Chem.* **2022**, *65*, 1-2.
22. Aldeen, T.S.; Mohamed, H.E.A.; Maaza, M. ZnO nanoparticles prepared via a green synthesis approach: Physical properties, photocatalytic and antibacterial activity. *J. Phys. Chem. Solids* **2020**, *160*, 110313.